

Inducible and Deterministic Forward Programming of Human Pluripotent Stem Cells into Neurons, Skeletal Myocytes, and Oligodendrocytes

Matthias Pawlowski,^{1,2,6,7,*} Daniel Ortmann,^{1,3,6} Alessandro Bertero,^{1,3,6,8} Joana M. Tavares,² Roger A. Pedersen,^{1,5} Ludovic Vallier,^{1,3,4} and Mark R.N. Kotter^{1,2,*}

¹Anne McLaren Laboratory, Wellcome Trust-MRC Stem Cell Institute, University of Cambridge, Cambridge CB2 0SZ, UK

²Department of Clinical Neuroscience, University of Cambridge, Cambridge CB2 0QQ, UK

³Department of Surgery, University of Cambridge, Cambridge CB2 0QQ, UK

⁴Wellcome Trust Sanger Institute, Hinxton, Cambridge CB10 1SA, UK

⁵Department of Paediatrics, University of Cambridge, Cambridge, CB2 0QQ, UK

⁶Co-first author

⁷Present address: Department of Neurology, University of Münster, 48149 Münster, Germany

⁸Present address: Department of Pathology, University of Washington, Seattle, WA 98109, USA

*Correspondence: pawlowski@uni-muenster.de (M.P.), mrk25@cam.ac.uk (M.R.N.K.)

<http://dx.doi.org/10.1016/j.stemcr.2017.02.016>

SUMMARY

The isolation or in vitro derivation of many human cell types remains challenging and inefficient. Direct conversion of human pluripotent stem cells (hPSCs) by forced expression of transcription factors provides a potential alternative. However, deficient inducible gene expression in hPSCs has compromised efficiencies of forward programming approaches. We have systematically optimized inducible gene expression in hPSCs using a dual genomic safe harbor gene-targeting strategy. This approach provides a powerful platform for the generation of human cell types by forward programming. We report robust and deterministic reprogramming of hPSCs into neurons and functional skeletal myocytes. Finally, we present a forward programming strategy for rapid and highly efficient generation of human oligodendrocytes.

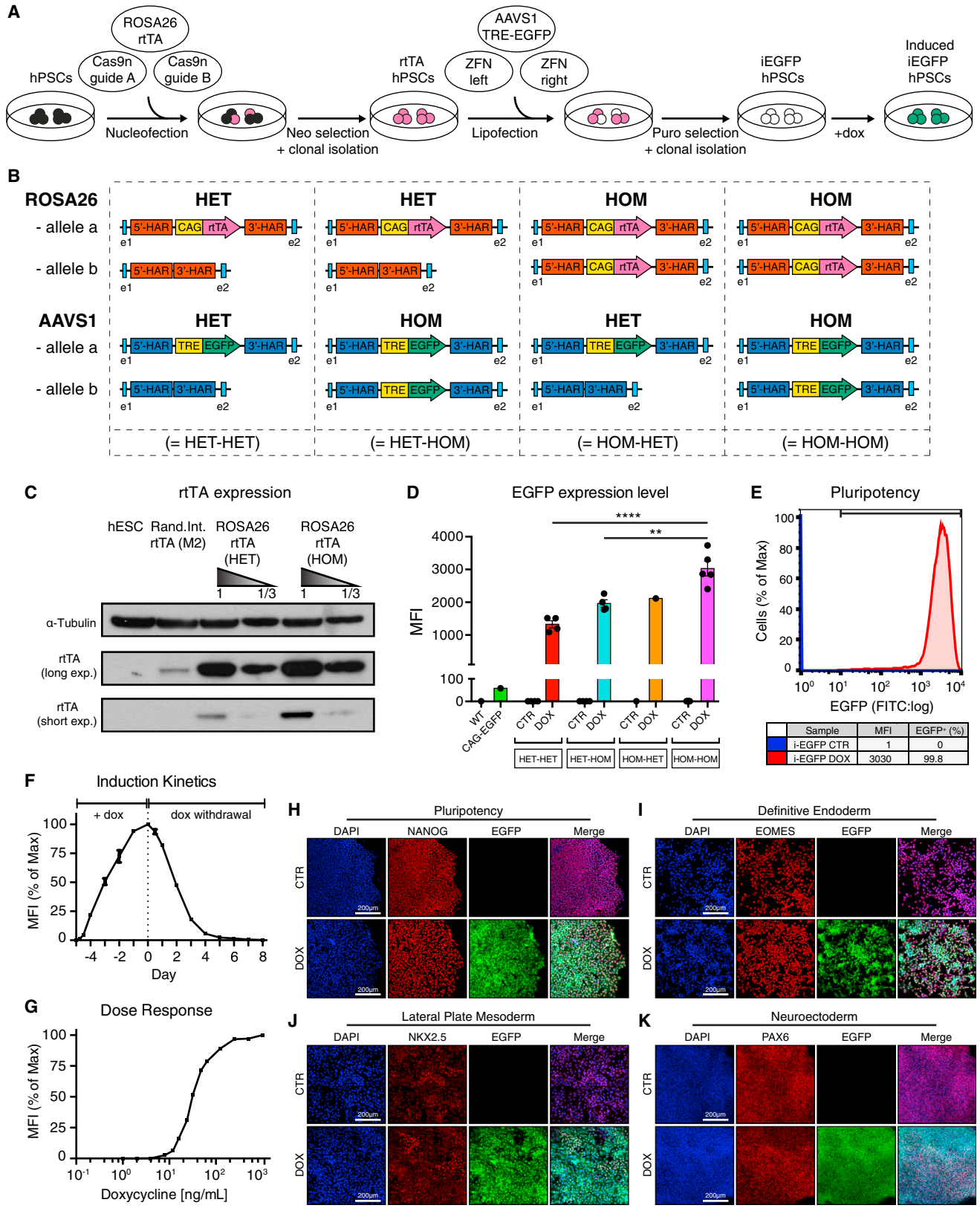
INTRODUCTION

Despite major efforts to develop robust protocols for scalable generation of human cell types from easily accessible and renewable sources, the differentiation of human pluripotent stem cells (hPSCs) into specific cell types often remains cumbersome, lengthy, and difficult to reproduce. Moreover, the recapitulation of developmental stages in vitro yields fetal cells that often do not reach full maturation (Cohen and Melton, 2011). More recently, forced expression of lineage-specific master regulators resulting in direct reprogramming of somatic cell types has provided an efficient alternative to directed differentiation (Huang et al., 2014; Ieda et al., 2010; Zhou et al., 2008). In particular, the direct conversion of hPSCs, termed forward programming (Moreau et al., 2016), combines the advantages of hPSC differentiation and direct cellular reprogramming, enabling scalable and rapid generation of human cell types (Zhang et al., 2013).

Currently available forward programming protocols are largely based on lentiviral transduction of hPSCs, which results in variegated expression or complete silencing of transgenes (Darabi et al., 2012; Smith et al., 2008). Additional purification steps are usually necessary for enriching the desired cell type. Lentiviral approaches randomly insert transgenes into the genome bearing the risk of unwanted interference with the endogenous transcriptional program. Therefore, refinements to the current forward programming approaches are desirable.

As the result of a systematic effort to optimize gene expression in hPSCs, we arrived at a robust hPSC forward programming platform by targeting all components of the Tet-ON system required for inducible expression of transcription factors into genomic safe harbor sites (GSHs) (Sadelain et al., 2012). The Tet-ON system consists of two components: a constitutively expressed transcriptional activator protein responsive to doxycycline (dox) (reverse tetracycline transactivator [rtTA]), and an inducible promoter regulated by rtTA (Tet-responsive element) that drives expression of the transgene (Baron and Bujard, 2000). Previous GSH-targeting strategies of the Tet-ON system relied on introducing both elements into the AAVS1 GSH of hPSCs, either separately (Hockemeyer et al., 2009), or together (using an all-in-one Tet-ON vector) (Ordovás et al., 2015; Qian et al., 2014). Compared with these designs, we reasoned that targeting each of the two elements of the Tet-ON system into a different GSH would have several advantages: inducible overexpression based on dual GSH targeting would not be affected by promoter interference between the two transgenes (Baron and Bujard, 2000), while homozygous GSH targeting would maximize the number of safely targeted transgene copies. Moreover, the larger cargo capacity in each of the transgenes would permit increased flexibility for transgene design, thus allowing the insertion of large reprogramming cassettes.

Here we show that an optimized approach based on dual GSH targeting of Tet-ON-controlled transgenes results in



(legend on next page)



homogeneous, controllable, and extremely high expression of inducible transgenes in hPSCs. Application of the optimized overexpression platform enabled us to develop rapid and deterministic forward programming protocols for mature human cell types.

RESULTS

Development of an Optimized Inducible Transgene Overexpression Method by Dual GSH Targeting

To optimize inducible transgene overexpression from GSHs, we generated human embryonic stem cells (hESCs) with inducible EGFP (i-EGFP) expression. Initially, we tested four different designs (Figure S1A). These comprised two all-in-one targeting constructs in which both rtTA and i-EGFP expression cassettes (third-generation Tet-ON system) were inserted into the same allele of the AAVS1 GSH locus. In these constructs, the rtTA expression was under the control of either an EF1 α or CAG promoter. The other two transgene designs were based on spatial separation of the activator and responder into two distinct GSHs (Figure S1A). For this purpose, we sequentially targeted the rtTA cassette into the human ROSA26 GSH (Bertero et al., 2016) and an i-EGFP transgene into the AAVS1 GSH (Figures 1A and S1A–S1E) (Hockemeyer et al., 2009). Robust and homogeneous inducible transgene expression was achieved only when the dual GSH approach and a CAG promoter for rtTA expression was used (Figure S1A). Importantly, the dual GSH-targeting approach was highly efficient (Table S1), and did not affect hESC self-renewal or differentiation (Figures 1H–1K).

Using the CAG promoter-based dual GSH-targeting approach, we selected clonal lines that carried either one

or two copies of each of the transgenes (Figure 1B), and observed that homozygous targeting of both elements allowed maximal inducible overexpression (Figures 1C, 1D, S1E, and S1F). Under these conditions, EGFP expression was induced homogeneously in all cells, consistent across multiple clones, and more than 50-fold higher compared with EGFP expression via the strong constitutive CAG promoter (Figures 1D, 1E, S1E, and S1F). Maximal EGFP levels were reached approximately 4 days after induction, and expression was quickly reversed upon dox withdrawal (Figure 1F). Moreover, EGFP expression could be titrated by adjusting the dose of dox (Figure 1G). I-EGFP expression was highly efficient in hESCs (Figures 1E and 1H), and during germ layer differentiation (Figures 1I–1K and S1G). There was no detectable background expression of EGFP in the absence of dox (Figures 1D, 1E, and S1G).

Taken together, these results established that homozygous dual GSH targeting of the Tet-ON system is a powerful strategy for homogeneous and controllable expression of inducible transgenes in hPSCs and their derivatives. We will refer to this platform as “OPTi-OX” (optimized inducible overexpression).

Human Induced Neurons

To test the applicability of the OPTi-OX platform for forward programming of hPSCs into mature cell types, we first chose to generate excitatory cortical neurons, as previous studies demonstrated that these can be readily derived by lentiviral overexpression of pro-neuronal transcription factors in hPSCs (Zhang et al., 2013).

To this end, we generated NGN2 OPTi-OX hPSCs (Figure 2A; Table S1), and treated them with dox in chemically defined neuronal culture medium (Zhang et al., 2013). Induction of NGN2 expression (Figure S2A) resulted in

Figure 1. Development of an Optimized Inducible Gene Overexpression System

(A) Workflow for targeting the hROSA26 and AAVS1 loci with the Tet-ON system in hPSCs for inducible EGFP expression (i-EGFP). Cas9n, D10A nickase mutant Cas9 endonuclease; ZFN, zinc-finger nucleases; rtTA, reverse tetracycline transactivator; TRE, Tet-responsive element.

(B) Schematic of the four outcomes following generation of dual GSH-targeted inducible EGFP hESCs: clonal lines were categorized based on the number of successfully targeted alleles of the hROSA26 and AAVS1 loci.

(C) Detection of the rtTA protein by western blot in heterozygous (HET) and homozygous (HOM) hROSA26-CAG-rtTA hESCs. Homozygous targeting results in increased rtTA protein expression. hESCs with random integration of a second-generation rtTA (M2-rtTA) and wild-type hESCs are shown as positive and negative reference. α -Tubulin, loading control.

(D) Median fluorescent intensity (MFI) of EGFP expression in the various dual GSH-targeted i-EGFP hESCs described in (B). Cells were analyzed by flow cytometry in non-induced conditions (CTR) or following 5 days of dox. AAVS1-CAG-EGFP and wild-type (WT) hESCs were included for comparison. Statistical analysis of dox-treated groups demonstrated that EGFP levels were highest in double-homozygous clones (each data point, $n = 1$ –5, represents a clonal line; mean \pm SEM; one-way ANOVA with post hoc Dunnett’s test; ** $p < 0.01$, **** $p < 0.0001$).

(E) Flow cytometry of EGFP OPTi-OX hESCs after 5 days of dox treatment. Non-induced cells were included as negative control.

(F and G) EGFP induction and rescue kinetics (F) and dox dose-response (G) in EGFP OPTi-OX hESCs detected by flow cytometry ($n = 2$ biological replicates; mean \pm SEM; all values normalized to the maximum fluorescence intensity after 5 days of dox).

(H–K) Immunocytochemistry (ICC) for lineage-specific markers in undifferentiated EGFP OPTi-OX hESCs and following differentiation into the germ layers.

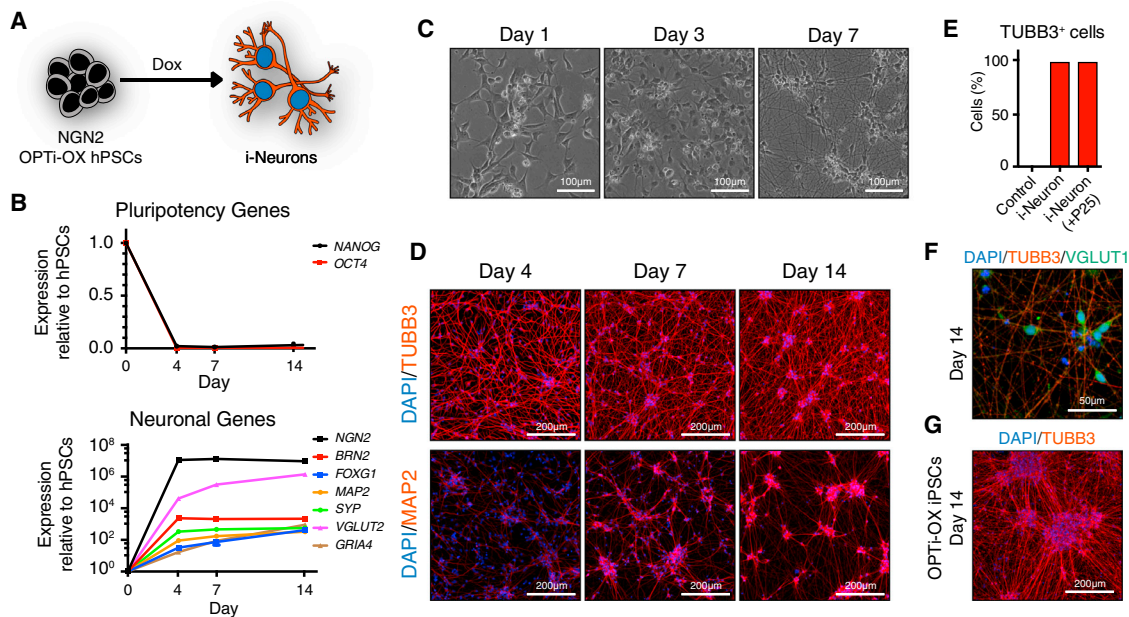


Figure 2. Forward Programming of hPSCs into Neurons

(A) Experimental approach for conversion of NGN2 OPTi-OX hPSCs into i-Neurons. (B) Time course of i-Neuron generation from hESCs by qPCR demonstrating the expression pattern of pluripotency factors (*OCT4* and *NANOG*), pan-neuronal (*MAP2* and *SYP*), forebrain (*BRN2*, *FOXG1*), and glutamatergic neuronal marker genes (*VGLUT2*, *GRIA4*) ($n = 3$ biological replicates; mean \pm SEM; relative to *PBGD* and normalized to pluripotency). (C) Phase contrast images illustrating the morphological changes during i-Neuron generation (a corresponding time-lapse is shown in [Movie S1](#)). (D) ICC for the pan-neuronal marker proteins β III-tubulin (TUBB3) and microtubule-associated protein 2 (MAP2) during the generation of i-Neurons. (E) Quantification of β III-tubulin-positive neuronal cells by ICC after 1 week of induction. Undifferentiated cells were used as negative control, and numbers are reported for i-Neuron generation in newly isolated NGN2 OPTi-OX hESCs and after 25 passages. (F and G) ICC for neuronal markers in i-Neurons 14 days after induction.

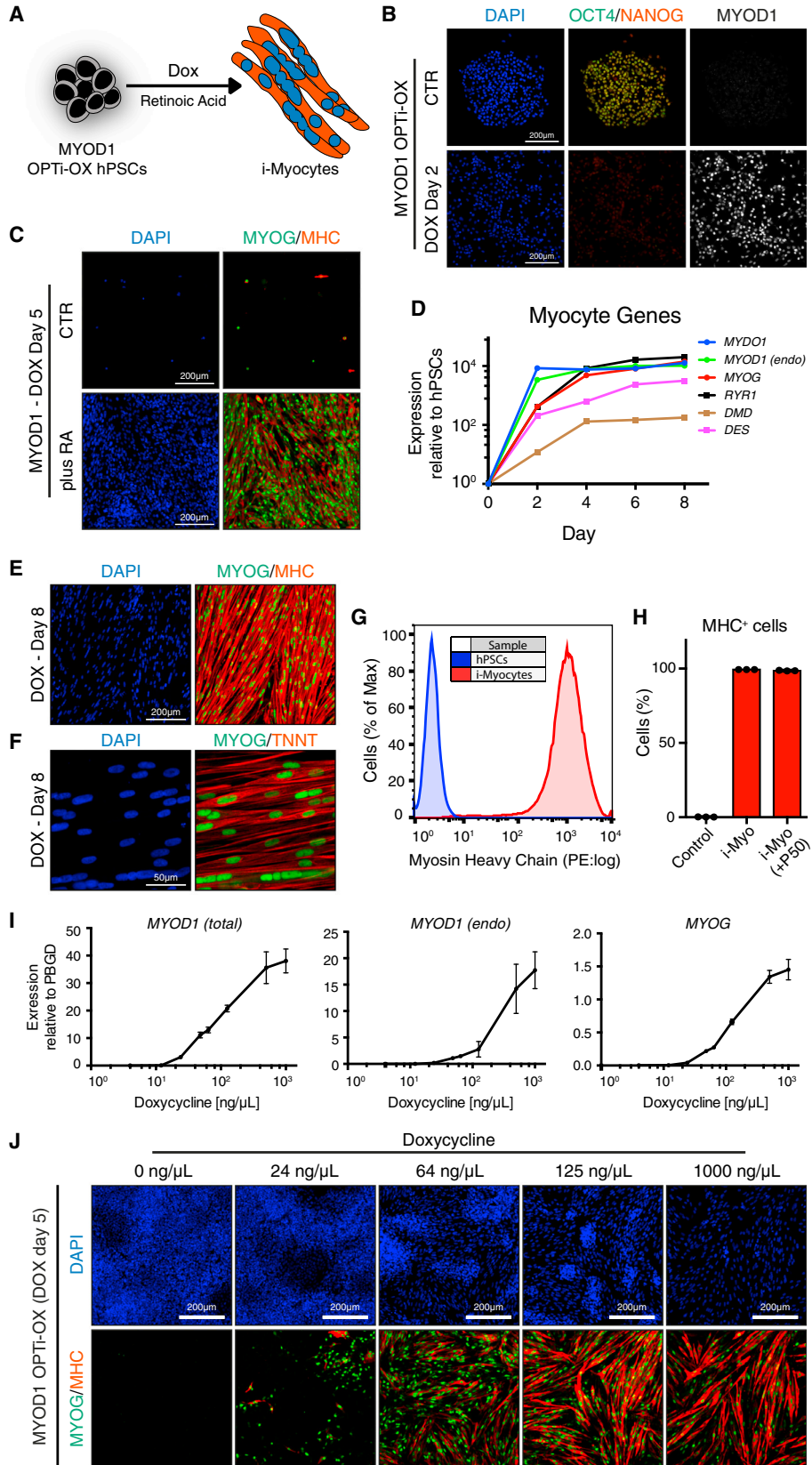
downregulation of pluripotency factors and initiation of the neuronal transcriptional program (Figure 2B). Dox-treated cells extended neuronal processes as early as 3 days post induction. After 1 week, all cells displayed a neuronal morphology and expressed the pan-neuronal markers β III-tubulin and MAP2 (Figures 2C–2E and [Movie S1](#)). At this stage, induced neurons (i-Neurons) showed strong expression of forebrain markers *BRN2* and *FOXG1*, and of glutamatergic neuronal genes *GRIA4*, *VGLUT1*, and *VGLUT2* (Figures 2B and 2F), indicative of an excitatory cortical neuronal identity of the forward-programmed cells, consistent with previous reports ([Zhang et al., 2013](#)). Short pulses of dox treatment for 4 days or longer sufficed for complete conversion, and converted cells did not rely on continuous transgene expression (Figures S2B and S2C). Importantly, we did not observe any reduction in the efficiency of generating i-Neurons over extended culture periods of the inducible hESCs (>25 passages, Figure 2E). Finally, we confirmed the applicability of the NGN2 OPTi-OX system in hiPSCs (Figure 2G).

Collectively, these results demonstrated that OPTi-OX enables robust and rapid forward programming of hPSCs into cortical neurons.

Human Induced Skeletal Myocytes

To further explore the potential of OPTi-OX for forward programming of hPSCs, we focused on generating human skeletal myocytes. Existing protocols for the directed differentiation of skeletal myocytes from hPSCs are difficult, time consuming, and result in low and variable yields ([Chal et al., 2015](#)). On the other hand, myogenic transdifferentiation has been achieved by overexpressing the transcription factor MYOD1 in somatic cell types, but the ability of hPSCs to undergo MYOD1-induced forward programming is a matter of debate ([Abujarour et al., 2014](#); [Albini et al., 2013](#); [Tanaka et al., 2013](#)).

We therefore generated MYOD1 OPTi-OX hPSCs (Figures 3A and 3B and [Table S1](#)). However, induction of MYOD1 expression following dox treatment resulted in cell death within 3–5 days, regardless of the culture medium used



(legend on next page)



(data not shown). These findings demonstrated that MYOD1 overexpression alone was not sufficient to drive myogenesis in hPSCs, in agreement with the postulated existence of epigenetic barriers preventing forced myogenesis (Albini et al., 2013).

Cellular reprogramming strategies can be enhanced by combining transcription factor overexpression with extracellular signaling cues (Bar-Nur et al., 2014). We conducted a systematic screen for pro-myogenic factors by modulating key signaling cascades that are implicated in primitive streak formation, somitogenesis, and myogenesis (Figure S3A). We found that the addition of all-*trans* retinoic acid (RA) in conjunction with MYOD1 overexpression was sufficient for rapid and deterministic conversion of hPSCs into myogenin and myosin heavy chain double-positive myocytes after 5 days of induction (Figures 3C and S3A). The effect of RA was concentration dependent (data not shown), and mediated at least in part through the receptor isoforms RAR α and RAR β (Figures S3B and S3C).

Following minor optimization of the culture conditions (see the Supplemental Experimental Procedures), we arrived at a protocol resulting in nearly pure induced skeletal myocytes (i-Myocytes). Reprogrammed cells developed typical spindle-like, elongated morphology, underwent extensive cell fusion, and exhibited strong and homogeneous myogenic marker expression on mRNA and protein levels (Figures 3D–3H, S3D, and S3E; Movie S2). Furthermore, the addition of nanomolar concentrations of acetylcholine (ACh) or the selective ACh-receptor agonist carbachol resulted in muscle fiber contraction, demonstrating the functionality of the i-Myocytes (Movie S3). Similar results were obtained with i-Myocytes generated from MYOD1 OPTi-OX hiPSCs (Figure S3F). Importantly, induction efficiency did not decrease over extended culture pe-

riods (>50 passages, Figure 3H), thus demonstrating the robustness and reproducibility of this method. Finally, we noted that the levels of the MYOD1 transgene following induction positively correlated with conversion efficiency (Figures 3I and 3J), which highlights the importance of a robust gene-delivery method. In conclusion, these data demonstrated that the OPTi-OX platform enables robust and rapid forward programming of hPSCs into skeletal myocytes.

Human Induced Oligodendrocytes

Encouraged by our results deriving neurons and myocytes, we sought to utilize the same overexpression system to develop a forward programming protocol for oligodendrocytes. Oligodendrocytes are of critical importance for CNS function and their loss or dysfunction plays a key role in many neurological diseases. Unlike neurons (Zhang et al., 2013), protocols for efficient generation of human oligodendrocytes from renewable sources remain an unmet need: currently available hPSC differentiation protocols are extremely long (up to 200 days) and yield heterogeneous cell populations (Douvaras et al., 2014; Stacpoole et al., 2013; Wang et al., 2013).

We generated OPTi-OX hPSCs bearing inducible SOX10 either alone or in combination with OLIG2 in the form of a polycistronic expression cassette (Figure 4A). Although cells induced with SOX10 alone robustly expressed the oligodendrocyte precursor (OPC) marker O4 after 10 days of induction, these cells failed to differentiate into myelin-expressing cells and died (Figure 4A). In contrast, the OLIG2-SOX10 overexpressing cells progressed from an O4-positive progenitor stage into a mature CNP/MBP-positive phenotype after 20 days of induction (Figure 4A). Moreover, gene expression analysis confirmed that OLIG2-SOX10 OPTi-OX hPSCs induced in oligodendrocyte

Figure 3. Forward Programming of hPSCs into Skeletal Myocytes

- (A) Experimental approach for rapid single-step conversion of MYOD1 OPTi-OX hPSCs into skeletal myocytes (i-Myocytes) following treatment with dox and RA.
- (B) Representative ICC for MYOD1 before (CTR) and after induction with dox. This demonstrates homogeneous induction of transgene expression, paralleled by downregulation of the pluripotency factors NANOG and OCT4.
- (C) Effect of RA on myocyte forward programming compared with otherwise identical control (CTR) induction conditions (see Figure S2B for the entire signaling molecule screen).
- (D) qPCR of the temporal expression pattern of pluripotency factors (top panel) and myocyte marker genes during i-Myocyte generation (n = 3 biological replicates, mean \pm SEM; relative to *PBGD* and normalized to pluripotency).
- (E and F) ICC for skeletal myocyte markers in i-Myocytes.
- (G and H) Quantification of MHC-positive cells by flow cytometry 10 days after induction. Undifferentiated cells were used as negative control, and figures are reported for i-Myocyte generation in newly isolated MYOD1 OPTi-OX hESCs, or in the same cells following 50 passages (+P50) (n = 3 biological replicates; mean \pm SEM).
- (I) qPCR for total *MYOD1*, endogenous *MYOD1*, and *MYOG* 2 days post induction with different dox concentrations (n = 3 biological replicates; mean \pm SEM).
- (J) ICC for myogenin and myosin heavy chain following 5 days of induction with different dox concentrations. Non-converted, proliferative cell clusters appeared when the dox concentration was lowered to 0.125 μ g/mL. Further reduction of dox resulted in an increase in non-myocyte cell populations.

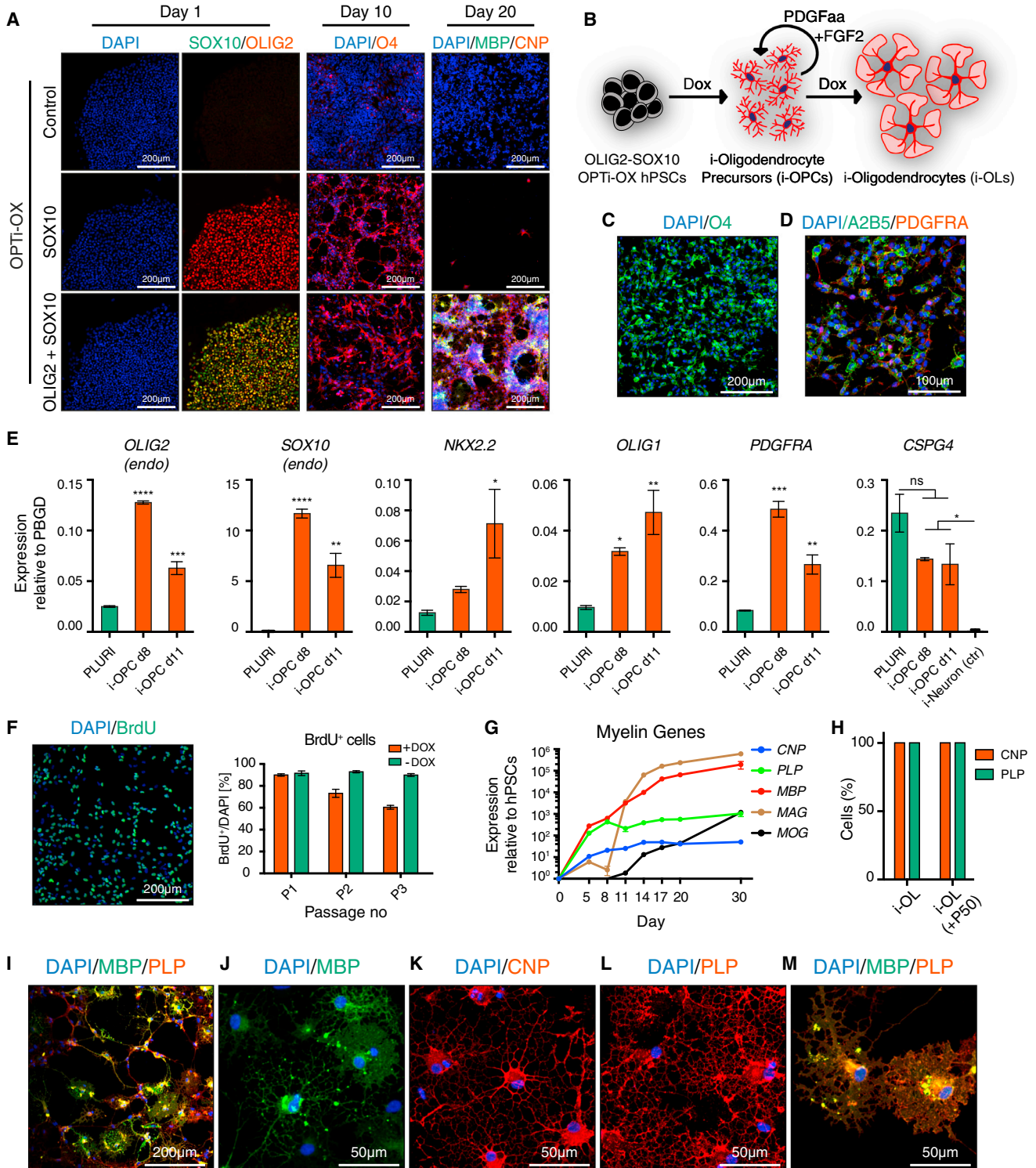


Figure 4. Forward Programming of hPSCs into Oligodendrocytes

(A) ICC for inducible transgenes after 1 day of induction (left column), the OPC marker O4 after 10 days (middle), and the oligodendrocyte markers CNP and MBP after 20 days (right).

(B) Experimental approach for rapid conversion of OLIG2-SOX10 OPTi-OX hPSCs into the oligodendrocyte lineage cells (i-OPCs and i-OLs).

(C and D) Characterization of i-OPCs by ICC for OPC surface markers (A2B5, O4, PDGFRA).

(legend continued on next page)



medium (Douvaras et al., 2014) supplemented with the mitogens PDGF α and FGF2 first passed through an OPC-like stage, during which they remained proliferative and co-expressed typical OPC markers (Figures 4B–4F). Remarkably, following withdrawal of mitogens, i-OPCs differentiated into mature oligodendrocytes, expressing the typical myelin-associated proteins (Figures 4G–4M).

DISCUSSION

OPTi-OX is the result of a systematic effort to optimize gene expression in hPSCs. It relies on a dual GSH-targeting strategy for the Tet-ON system, overcoming the limitations of viral-mediated transgene delivery forward programming protocols (Abujarour et al., 2014; Darabi et al., 2012; Zhang et al., 2013) and allows stronger and more controlled transgene overexpression compared with previous targeting approaches (González et al., 2014; Hockemeyer et al., 2009; Ordovás et al., 2015). Table S2 compares the gene-delivery methods that have been used for transcription factor expression in different hPSC forward programming approaches. Moreover, site-specific insertion of the two components of the inducible gene expression system minimizes genomic off-target effects and together with the chemically defined medium compositions enhances the reproducibility of the protocols.

The functionality of our platform is exemplified through the production of several cell types. First, we show that NGN2 and MYOD1 OPTi-OX hPSCs can be used as an inexhaustible source for highly scalable, rapid, single-step, virus-free, chemically defined, fully reproducible, and deterministic generation of i-Neurons and i-Myocytes.

Finally, we successfully applied the OPTi-OX platform to develop a forward programming protocol for generating human oligodendrocytes. Recent studies demonstrated that forced expression of transcription factors allows direct conversion of rodent fibroblasts (Najm et al., 2013; Yang et al., 2013), and primary human fetal neural stem cells (Wang et al., 2014) into OPCs, but the reprogramming of

renewable human cell sources into oligodendrocytes has not been reported. While i-OPCs undergo the expected morphological changes, and express mature markers in monocultures in vitro, further characterization of the cells using co-culture models and transplantation into myelin-deficient mutants is needed.

Human oligodendrocytes are of considerable interest for several applications. The efficiency and speed of the presented forward programming system will enable high-throughput drug screens and toxicology testing, in vitro modeling of hereditary leukodystrophies, and the development of cell-transplantation strategies (Goldman et al., 2012).

Transcription factor combinations for direct cellular reprogramming into many cell types of clinical interest are now available, including cardiomyocytes (Ieda et al., 2010), pancreatic β cells (Zhou et al., 2008), and hepatocytes (Huang et al., 2014). We anticipate that the OPTi-OX platform will be applicable for the generation of many other cell types. Overall, the presented method can provide the basis for inexhaustible, high-throughput, homogeneous, and large-scale manufacturing of many human cell types.

EXPERIMENTAL PROCEDURES

Gene Targeting

Targeting of the hROSA26 and AAVS1 locus was performed as described recently (Bertero et al., 2016). Targeting of the hROSA26 locus was done by nucleofection. Neomycin-resistant colonies were picked and screened by genotyping. Correctly hROSA26-rtTA-targeted clones were subsequently targeted with the inducible transgene cassette in the AAVS1 locus by lipofection. Resulting puromycin-resistant colonies were picked and re-analyzed by genotyping.

Inducible Transgene Expression and Forward Programming

Inducible overexpression was performed with dual GSH-targeted OPTi-OX hPSCs. Expression of inducible transgenes was prompted

(E) Characterization of i-OPCs by qPCR compared with hPSCs (PLURI). As transcription of *CSPG4* (NG2) was also detected in hPSCs, we included i-Neurons as negative control (n = 3 biological replicates; mean \pm SEM; all values relative to *PBGD*; one-way ANOVA with post hoc Dunnett's test; *p < 0.05; **p < 0.01, ***p < 0.001, ****p < 0.0001; ns, p > 0.05).

(F) Immunostaining for BrdU (left panel) and quantification of BrdU-positive cells following three serial passages of i-OPCs every 4 days and concomitant BrdU-pulses (n = 3 biological replicates; mean \pm SEM; P, passage).

(G) qPCR of the temporal expression pattern of genes encoding for the myelin-associated proteins (*CNP*, *MAG*, *MBP*, *MOG*, and *PLP*) during i-OL generation. OLIG2-SOX10 OPTi-OX hPSCs were induced in oligodendrocyte medium supplemented with PDGF α and FGF2. After 1 week of induction, mitogens were withdrawn to enable terminal differentiation (n = 3 biological replicates; mean \pm SEM; all values relative to *PBGD* and normalized to pluripotency).

(H) Quantification of CNP and PLP expressing i-OLs derived from OLIG2-SOX10 OPTi-OX hPSCs after 20 days of induction by ICC. Undifferentiated cells were used as negative control, and figures are reported for newly isolated OLIG2-SOX10 OPTi-OX hPSCs and after 50 passages (+P50).

(I–M) ICC providing an overview (I) and high-magnifications (J–M) of mature pre-myelinating oligodendrocytes.



by adding dox to the culture medium. For forward programming into neurons, skeletal myocytes, and oligodendrocytes, standard medium conditions for the derivation of the respective cell types were used. Gene and protein expression analysis was performed as described recently (Bertero et al., 2016). Please refer to the [Supplemental Experimental Procedures](#) for details on culture conditions and analysis techniques.

SUPPLEMENTAL INFORMATION

Supplemental Information includes Supplemental Experimental Procedures, three figures, two tables, and three movies and can be found with this article online at <http://dx.doi.org/10.1016/j.stemcr.2017.02.016>.

AUTHOR CONTRIBUTIONS

M.P. conceived the study, designed and performed experiments, analyzed data, and wrote the first draft of the manuscript. D.O. designed and performed experiments and analyzed the data. A.B. designed and performed experiments, analyzed data, and wrote the manuscript. J.M.T. performed additional experiments. R.A.P. provided expert advice. L.V. supervised and supported the study. M.R.N.K. conceived, supervised, supported the study, and finalized the manuscript.

ACKNOWLEDGMENTS

We thank Kosuke Yusa for providing the AAVS1 ZFN plasmids. Research in the senior author's laboratory is supported by a core support grant from the Wellcome Trust and MRC to the Wellcome Trust-Medical Research Council Cambridge Stem Cell Institute. Further support was provided by a research fellowship from the German Research Foundation (DFG PA2369/1-1 to M.P.), a British Heart Foundation PhD Studentship (FS/11/77/39327 to A.B.), a Clinician Scientist Award from the National Institute for Health Research UK (CS-2015-15-023 to M.R.N.K.), and the Qatar Foundation (to M.R.N.K.). The Wellcome Trust – Medical Research Council Cambridge Stem Cell Institute is supported by core funding from the Wellcome Trust and MRC. The views expressed in this publication are those of the authors and not necessarily those of the NHS, the National Institute for Health Research or the Department of Health. Patent protection has been sought for the dual/multiple safe harbour site approach and individual reprogramming protocols detailed in the present manuscript.

Received: June 13, 2016

Revised: February 17, 2017

Accepted: February 17, 2017

Published: March 23, 2017

REFERENCES

Abujarour, R., Bennett, M., Valamehr, B., Lee, T.T., Robinson, M., Robbins, D., Le, T., Lai, K., and Flynn, P. (2014). Myogenic differentiation of muscular dystrophy-specific induced pluripotent stem cells for use in drug discovery. *Stem Cells Transl. Med.* *3*, 149–160.

Albini, S., Coutinho, P., Malecova, B., Giordani, L., Savchenko, A., Forcales, S.V., and Puri, P.L. (2013). Epigenetic reprogramming of

human embryonic stem cells into skeletal muscle cells and generation of contractile myospheres. *Cell Rep.* *3*, 661–670.

Bar-Nur, O., Brumbaugh, J., Verheul, C., Apostolou, E., Pruteanu-Malinici, I., Walsh, R.M., Ramaswamy, S., and Hochedlinger, K. (2014). Small molecules facilitate rapid and synchronous iPSC generation. *Nat. Methods* *11*, 1170–1176.

Baron, U., and Bujard, H. (2000). Tet repressor-based system for regulated gene expression in eukaryotic cells: principles and advances. *Methods Enzymol.* *327*, 401–421.

Bertero, A., Pawlowski, M., Ortmann, D., Snijders, K., Yiangou, L., Cardoso de Brito, M., Brown, S., Bernard, W.G., Cooper, J.D., Giacomelli, E., et al. (2016). Optimized inducible shRNA and CRISPR/Cas9 platforms for in vitro studies of human development using hPSCs. *Development* *143*, 4405–4418.

Chal, J., Oginuma, M., Al Tanoury, Z., Gobert, B., Sumara, O., Hick, A., Bousson, F., Zidouni, Y., Mursch, C., Moncuquet, P., et al. (2015). Differentiation of pluripotent stem cells to muscle fiber to model Duchenne muscular dystrophy. *Nat. Biotechnol.* *33*, 962–969.

Cohen, D.E., and Melton, D.A. (2011). Turning straw into gold: directing cell fate for regenerative medicine. *Nat. Rev. Genet.* *12*, 243–252.

Darabi, R., Arpke, R.W., Irion, S., Dimos, J.T., Grskovic, M., Kyba, M., and Perlingeiro, R.C.R. (2012). Human ES- and iPS-derived myogenic progenitors restore DYSTROPHIN and improve contractility upon transplantation in dystrophic mice. *Cell Stem Cell* *10*, 610–619.

Douvaras, P., Wang, J., Zimmer, M., Hanchuk, S., O'Bara, M.A., Sadiq, S., Sim, F.J., Goldman, J., and Fossati, V. (2014). Efficient generation of myelinating oligodendrocytes from primary progressive multiple sclerosis patients by induced pluripotent stem cells. *Stem Cell Rep.* *3*, 250–259.

Goldman, S.A., Nedergaard, M., and Windrem, M.S. (2012). Glial progenitor cell-based treatment and modeling of neurological disease. *Science* *338*, 491–495.

González, F., Zhu, Z., Shi, Z.D., Lelli, K., Verma, N., Li, Q.V., and Huangfu, D. (2014). An iCRISPR platform for rapid, multiplexable, and inducible genome editing in human pluripotent stem cells. *Cell Stem Cell* *15*, 215–226.

Hockemeyer, D., Soldner, F., Beard, C., Gao, Q., Mitalipova, M., DeKaveler, R.C., Katibah, G.E., Amora, R., Boydston, E.A., Zeitler, B., et al. (2009). Efficient targeting of expressed and silent genes in human ESCs and iPSCs using zinc-finger nucleases. *Nat. Biotechnol.* *27*, 851–857.

Huang, P., Zhang, L., Gao, Y., He, Z., Yao, D., Wu, Z., Cen, J., Chen, X., Liu, C., and Hu, Y. (2014). Direct reprogramming of human fibroblasts to functional and expandable hepatocytes. *Cell Stem Cell* *14*, 370–384.

Ieda, M., Fu, J.-D., Delgado-Olguin, P., Vedantham, V., Hayashi, Y., Bruneau, B.G., and Srivastava, D. (2010). Direct reprogramming of fibroblasts into functional cardiomyocytes by defined factors. *Cell* *142*, 375–386.

Moreau, T., Evans, A.L., Vasquez, L., Tijssen, M.R., Yan, Y., Trotter, M.W., Howard, D., Colzani, M., Arumugam, M., Wu, W.H., et al. (2016). Large-scale production of megakaryocytes from human



- pluripotent stem cells by chemically defined forward programming. *Nat. Commun.* **7**, 11208.
- Najm, F.J., Lager, A.M., Zaremba, A., Wyatt, K., Caprariello, A.V., Factor, D.C., Karl, R.T., Maeda, T., Miller, R.H., and Tesar, P.J. (2013). Transcription factor-mediated reprogramming of fibroblasts to expandable, myelinogenic oligodendrocyte progenitor cells. *Nat. Biotechnol.* **31**, 426–433.
- Ordovás, L., Boon, R., Pistoni, M., Chen, Y., Wolfs, E., Guo, W., Sambathkumar, R., Bobis-Wozowicz, S., Helsen, N., Vanhove, J., et al. (2015). Efficient recombinase-mediated cassette exchange in hPSCs to study the hepatocyte lineage reveals AAVS1 locus-mediated transgene inhibition. *Stem Cell Rep.* **5**, 918–931.
- Qian, K., Huang, C.-L., Chen, H., Blackbourn, L.W., Chen, Y., Cao, J., Yao, L., Sauvey, C., Du, Z., and Zhang, S.-C. (2014). A simple and efficient system for regulating gene expression in human pluripotent stem cells and derivatives. *Stem Cells* **32**, 1230–1238.
- Sadelain, M., Papapetrou, E.P., and Bushman, F.D. (2012). Safe harbours for the integration of new DNA in the human genome. *Nat. Rev. Cancer* **12**, 51–58.
- Smith, J.R., Maguire, S., Davis, L.A., Alexander, M., Yang, F., Chandran, S., Ffrench-Constant, C., and Pedersen, R.A. (2008). Robust, persistent transgene expression in human embryonic stem cells is achieved with AAVS1-targeted integration. *Stem Cells* **26**, 496–504.
- Stacpoole, S.R.L., Spitzer, S., Bilican, B., Compston, A., Karadottir, R., Chandran, S., and Franklin, R.J.M. (2013). High yields of oligodendrocyte lineage cells from human embryonic stem cells at physiological oxygen tensions for evaluation of translational biology. *Stem Cell Rep.* **1**, 437–450.
- Tanaka, A., Woltjen, K., Miyake, K., Hotta, A., Ikeya, M., Yamamoto, T., Nishino, T., Shoji, E., Sehara-Fujisawa, A., Manabe, Y., et al. (2013). Efficient and reproducible myogenic differentiation from human iPSC cells: prospects for modeling Miyoshi myopathy in vitro. *PLoS One* **8**, e61540.
- Wang, S., Bates, J., Li, X., Schanz, S., Chandler-Militello, D., Levine, C., Maherali, N., Studer, L., Hochedlinger, K., Windrem, M., et al. (2013). Human iPSC-derived oligodendrocyte progenitor cells can myelinate and rescue a mouse model of congenital hypomyelination. *Cell Stem Cell* **12**, 252–264.
- Wang, J., Pol, S.U., Haberman, A.K., Wang, C., O'Bara, M.A., and Sim, F.J. (2014). Transcription factor induction of human oligodendrocyte progenitor fate and differentiation. *Proc. Natl. Acad. Sci. USA* **111**, E2885–E2894.
- Yang, N., Zuchero, J.B., Ahlenius, H., Marro, S., Ng, Y.H., Vierbuchen, T., Hawkins, J.S., Geissler, R., Barres, B.A., and Wernig, M. (2013). Generation of oligodendroglial cells by direct lineage conversion. *Nat. Biotechnol.* **31**, 434–439.
- Zhang, Y., Pak, C., Han, Y., Ahlenius, H., Zhang, Z., Chanda, S., Marro, S., Patzke, C., Acuna, C., Covy, J., et al. (2013). Rapid single-step induction of functional neurons from human pluripotent stem cells. *Neuron* **78**, 785–798.
- Zhou, Q., Brown, J., Kanarek, A., Rajagopal, J., and Melton, D.A. (2008). In vivo reprogramming of adult pancreatic exocrine cells to beta-cells. *Nature* **455**, 627–632.

Stem Cell Reports, Volume 8

Supplemental Information

Inducible and Deterministic Forward Programming of Human Pluripotent Stem Cells into Neurons, Skeletal Myocytes, and Oligodendrocytes

Matthias Pawlowski, Daniel Ortmann, Alessandro Bertero, Joana M. Tavares, Roger A. Pedersen, Ludovic Vallier, and Mark R.N. Kotter

Supplemental Figures

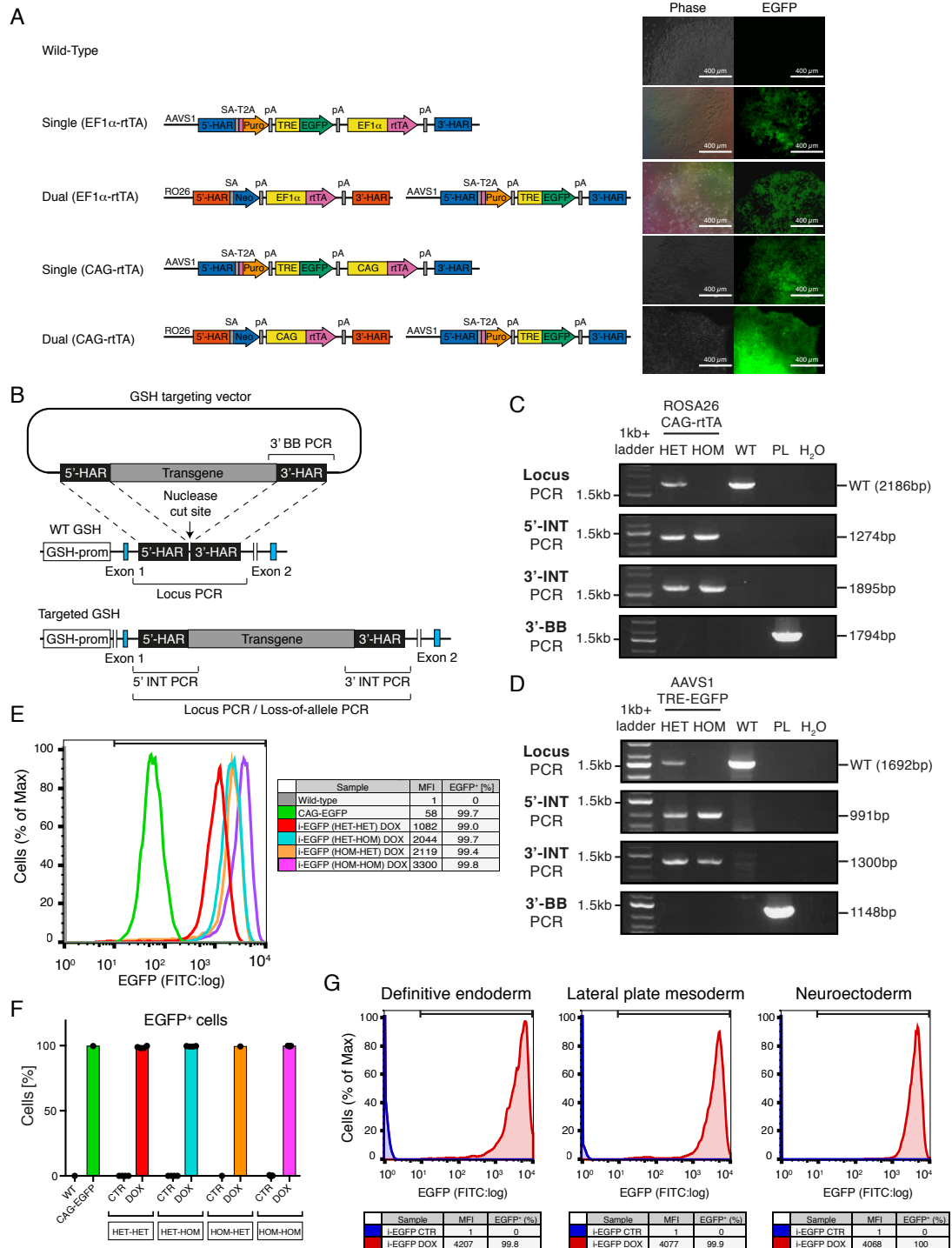


Figure S1. Related to Figure 1: Generation of hPSCs with inducible EGFP expression

(A) Schematic of the four different GSH (hROSA26 and AAVS1) targeting strategies: the two components (rtTA trans-activator cassette and inducible TRE-EGFP responder cassette) of the Tet-ON system were targeted either separately into the hROSA26 and AAVS1 locus, respectively, or together into the same allele of the AAVS1 locus by using an all-in-one donor vector design. For both configurations rtTA expression is controlled either by an EF1 α - or CAG-promoter. The resulting cell lines were treated with dox for 5 days. Phase contrast and EGFP-images demonstrate homogeneous EGFP expression only in the dual GSH-targeting strategy in which rtTA expression is under control of the CAG promoter. Abbreviations: *RO26*: human ROSA26 (hROSA26) locus; *AAVS1*: AAVS1 locus; 5'-HAR/3'-HAR: upstream/downstream homology arm. *SA*: splice acceptor; *T2A*: T2A peptide

(ribosomal skipping signal); *Neo*: neomycin resistance gene (neomycin phosphotransferase II); *Puro*: puromycin resistance gene (puromycin *N*-acetyltransferase); *pA*: polyadenylation signal; *EF1 α* : human elongation factor 1 α promoter; *CAG*: CMV early enhancer, chicken β -actin and rabbit β -globin hybrid promoter; *EGFP*: enhanced green fluorescent protein; *CAG*: **(B)** Schematic of the genotyping strategy used to identify correctly targeted hROSA26 and AAVS1 targeted hPSC lines. *GSH-prom*: hROSA26 and AAVS1 promoter, respectively; *WT*: wild-type; *Transgene*: entire exogenous sequence integrated following targeting. *Locus PCR*: PCR spanning the targeted locus with both primers binding exclusively to genomic DNA outside the genomic sequence corresponding to the homology arms. Note that due to its high GC-content the *CAG* promoter cannot be amplified by routine PCR. Therefore, correct insertion of the *CAG*-containing expression cassette results in loss of a PCR amplicon. The presence of the wild-type band indicates the presence of non-targeted alleles, and loss of the wild-type band indicates homozygous targeting. *5'-INT/3'-INT PCRs*: PCRs spanning the 5'- and 3'-insertion site, respectively. Correctly sized PCR amplicons indicate correct integration. *3'-BB PCR*: PCR spanning the homology arm/targeting vector backbone junction. The presence of a PCR product indicates non-specific off-target integration of the donor plasmid. **(C-D)** Genotyping results for selected hROSA26-CAG-rtTA targeted (C) and AAVS1-TRE-EGFP re-targeted hPSCs (D). Heterozygous (HET) and homozygous (HOM) lines for each allele are shown. *1kb+*: 1kb plus DNA ladder; *WT*: wild-type hPSCs; *PL*: targeting plasmid; *H₂O*: water control. Refer to Supplemental Table 1 for a summary of all genotyping results and Supplemental Table 2 for the sequence of all genotyping primers. **(E)** Representative flow cytometry analysis of the various dual GSH-targeted inducible EGFP hPSCs described in figure 1B. Cells were analyzed in control conditions (no dox, CTR) or following 5 days of dox treatment (DOX). An hESC line in which EGFP expression is under control of a *CAG* promoter in the AAVS1 locus (Bertero et al. 2016) is included as a positive control and for comparison. Note that the FITC (EGFP) acquisition settings were set to enable plotting of the highest levels of EGFP expression. Thus, the negative control (wild-type) is located directly adjacent to the left y-axis. **(F)** Percentage of EGFP positive cells in the various dual GSH-targeted inducible EGFP hESCs (each data point represents an individual clonal line; n=1-5) **(G)** Representative EGFP flow cytometry plots in EGFP OPTi-OX hPSCs that were differentiated into the three germ layers. EGFP was induced with dox for the duration of the differentiation protocol (3 to 6 days, refer to Supplemental Methods).

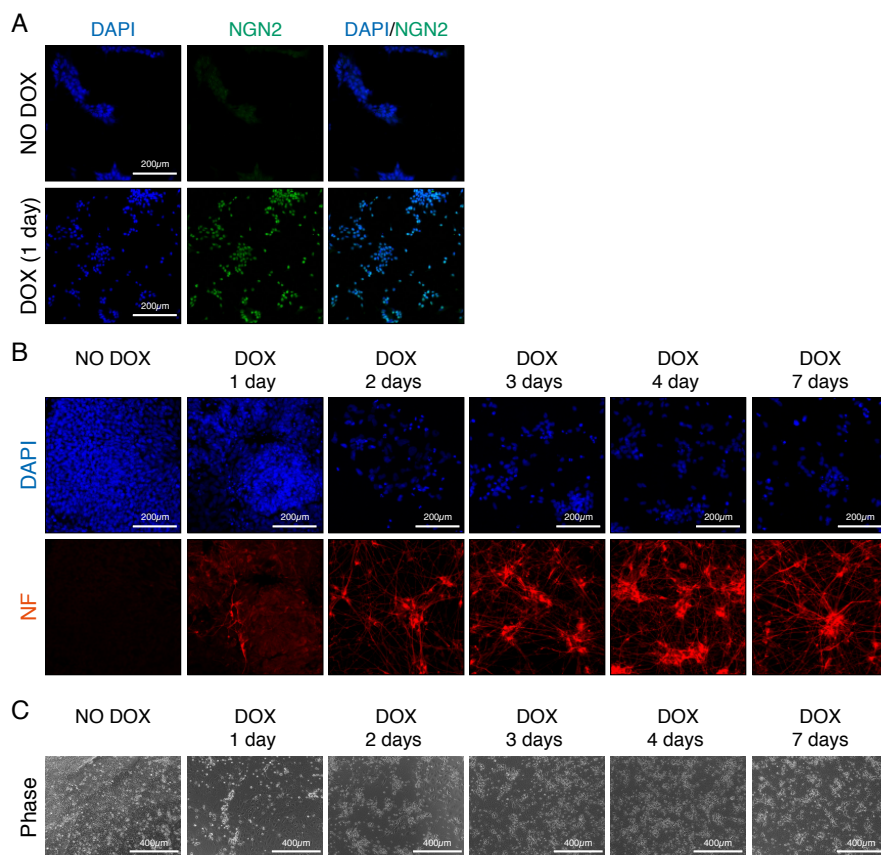


Figure S2. Related to Figure 2: Characterization of induced neurons

(A) Representative immunocytochemistry for NGN2 in NGN2 OPTi-OX hPSCs before (NO DOX) and 24h after induction with dox (DOX). The staining demonstrates robust and homogeneous induction of transgene expression. **(B)** Representative immunocytochemistry for the pan-neuronal marker neurofilament (NF) 7 days after the start of induction with dox. NGN2 OPTi-OX hPSCs were treated with doxycycline for 0, 1, 2, 3, 4 or 7 days, respectively. A minimum of 4 days of dox treatment was sufficient to yield the same number of neurons compared to the addition of dox supplementation throughout the experiment. **(C)** Representative phase contrast images of the same cultures shown in panel B.

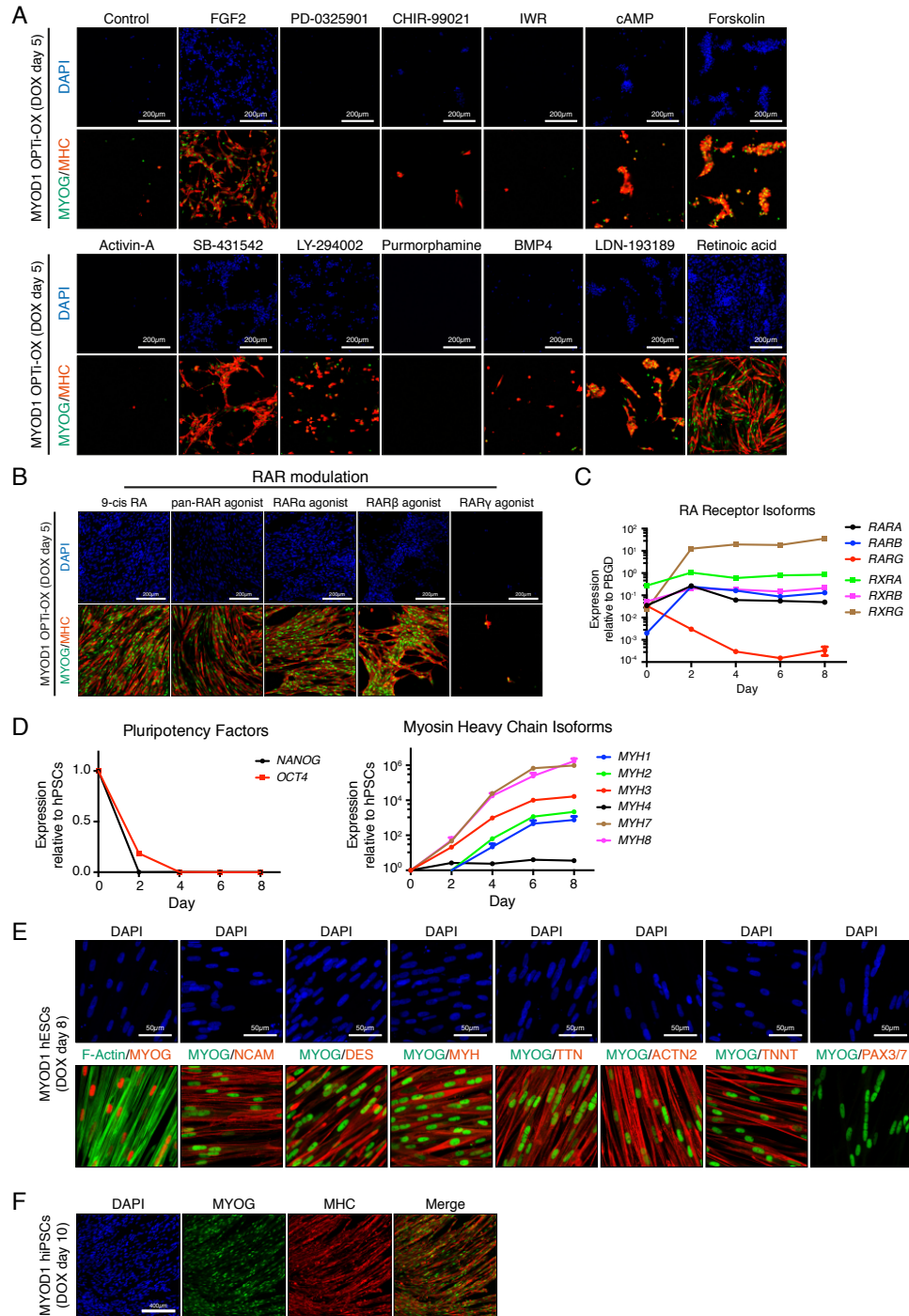


Figure S3. Related to Figure 3: Screening for chemically-defined culture conditions for the induction of skeletal myocytes and characterization of skeletal myocytes

(A) Screening for pro-myogenic factors: MYOD1 overexpression was initiated in DMEM basal media supplemented with different modulators of signaling cascades implicated in mesoderm patterning, somitogenesis and myogenesis. Shown is the immunocytochemistry for the myocyte markers myogenin (MYOG) and myosin heavy chains (MYH) 5 days post induction. This screen suggested that FGF2, forskolin (an adenylyl cyclase activator), and SB-431542 (an Activin/Nodal signaling inhibitor) have minor beneficial effects on cell survival and induction of myogenin and myosin heavy chain. However, the addition of all-trans retinoic acid (RA) led to the best outcome regarding survival, cell morphology and marker expression. This culture condition was chosen for the generation of induced myocytes (i-Myocytes) from MYOD1 OPTi-OX hPSCs. **(B)** RA was replaced with a range of selective, isoform-specific RA-Receptor agonists throughout the myocyte induction protocol (pan-RAR/RXR agonist: 9-cis RA 1 μ M; pan-RAR agonist: TTNPB 1 μ M; RAR α agonist: BMS753 1 μ M; RAR β agonist: CD2314 1 μ M; RAR γ agonist: BMS961 1 μ M). Immunocytochemistry for myogenin and myosin heavy chain 5 days post induction demonstrated that the enhancing effect of RA during myocyte induction are mediated through the RA receptor isoforms RAR α and RAR β , but not RAR γ . **(C)** qPCR analysis of the six retinoid and rexinoid receptors during myocyte induction demonstrated expression of RAR α , RAR β and all three RXR isoforms, but not of RAR γ throughout the course of i-Myocyte generation, consistent with the expression pattern of RA receptors during developmental myogenesis (n=3 biological replicates; mean \pm SEM). **(D)** qPCR analysis of pluripotency factors and myosin heavy chain (MHC) isoforms during myocyte induction demonstrated rapid downregulation of the pluripotency factors *NANOG* and *OCT4* (left panel), and strong upregulation of all major human skeletal myocyte-specific MHC isoforms (encoded by the *MYH* gene family) during i-Myocyte generation. The upregulated MHC-isoforms included the two isoforms that are expressed during embryonic and postnatal muscle development (embryonic isoform MYH3; neonatal isoform MYH8), and three isoforms that are expressed in adult human skeletal muscle [MYH7 in slow-twitching (type I) fibers; MYH2 in fast-twitching fatigue-resistant (type IIa) fibers, and MYH1 in fast-fatigable (type IIx) fibers]. In contrast, MYH4 which represents the constituting MHC-isoform in fast-twitching, fast-fatigable myocyte fibers in cats is not expressed in significant amounts in humans (<1%) and is also not induced throughout the forward programming time course (n=3 biological replicates; mean \pm SEM). **(E)** i-Myocytes express a broad range of typical marker proteins, including F-actin (visualized through AlexaFluor488-conjugated Phalloidin toxin), neural cell adhesion molecule (*NCAM*), desmin (*DES*), myosin heavy chains (*MYH*), titin (*TTN*), α -actinin (*ACTN2*) and troponin T (*TNNT*), but not the myoblast progenitor markers *PAX3* and *PAX7*. All samples were co-stained with myogenin. **(F)** Human MYOD1 OPTi-OX hiPSCs underwent myogenic induction comparably to their hESC counterparts, as demonstrated by immunocytochemistry for myogenin and myosin heavy chain 10 days post induction.

Supplemental Tables

Table S1. Summary of genotyping results

Locus	Cell-Line	Trans-gene	# clones picked (a)	# clones no on-tar. Integrat. (b)	# clones HET + off-targ. (c)	# clones HOM +off-targ. (e)	# clones HET (d)	# clones HOM (d)	Efficiency no off-tar. [%] (e)	Efficiency total [%] (f)
ROSA26	H9	rtTA	23/27/60*	2/3/1*	7/13/36*	5/3/6*	8/8/14*	1/0/3*	39/30/28*	91/89/98*
ROSA26	iPSC	rtTA	48	8	11	2	25	2	56	83
AAVS1	H9	EGFP	12/12/24*	2/1/2*	0/0/0*	4/5/11*	0/1/4*	6/5/7*	50/50/46*	83/92/92*
AAVS1	H9	NGN2	6	0	0	0	0	6	100	100
AAVS1	iPSC	NGN2	3	0	0	2	1	0	33	100
AAVS1	H9	MYOD1	12	2	0	3	0	7	58	75
AAVS1	iPSC	MYOD1	3	0	1	1	0	1	33	100

Refer to Figure S1B for a schematic and additional explanations of the PCR genotyping strategy used.

(a) Number of clones that were picked for expansion and genotyping following nucleofection (for hROSA26 targeting) and lipofection (for AAVS1 targeting), respectively. The total numbers of drug resistant colonies (from which the stated numbers of colonies were picked) were approximately 200 colonies per 10cm dish following nucleofection, and 20 colonies per well of 6-well plate following lipofection.

(b) Incorrect targeting: No evidence of targeting (lack of bands in 5'- and 3'-integration PCR and presence of WT band in locus PCR) or evidence of targeting, but incorrect size of 5'- or 3'-integration PCR.

(c) Correct on-target integration with additional random integration of the plasmid (bands in 3'-backbone PCR).

(d) Correct on-target integration (HET, heterozygous; HOM, homozygous).

(e) Percentage of clones with correct on-target integration (without additional off-target integration).

(f) Percentage of clones with correct on-target integration (with or without additional off-target integration).

* The three numbers are from three different targeting experiments in hESCs.

Table S2. Overview of gene delivery strategies in forward programming experiments

Gene Delivery	Off-switch (a)	Resistance to Silencing (b)	Expression level (c)	Genomic homogeneity /integrity of targeted cells (d)	Independency of optimized viral transduction (e)	Reproducibility (f)	Reference
*acute Lenti PGK	0	+	+	0	0	+	Albini et al. 2013
*acute Lenti EF1 α	0	+	+	0	0	+	Moreau et al. 2016
*acute Lenti i-TRE	+	+	0	0	0	+	Pang et al. 2011
*acute Lenti i-TRE (select)	+	++	++	0	+	++	Zhang et al. 2013
**clonal Lenti/Pig i-TRE	+	++	+	+	++	0	Abujarour et al. 2014 Tanaka et al. 2013
Single GSH i-TRE	++	++	++	+++	+++	+++	This study
Dual GSH i-TRE	+++	+++	+++	+++	+++	+++	This study

*acute: hPSCs are transduced with lentiviral vectors (Lenti) - encoding either a constitutive or inducible reprogramming factor expression cassette - at the beginning of each individual reprogramming experiment.

**clonal: hPSCs are transduced with lentiviral vectors (Lenti) or piggyback vectors (Pig) – encoding an inducible reprogramming factor cassette – clonally expanded, and each clonal line is subsequently analyzed for its transgene expression and forward programming capacity.

(a) An optimal gene delivery system for forward programming contains an on-/off-switch to allow for controlled transcription factor expression during the reprogramming process and turning-off after a full cellular conversion has been achieved. This cannot be achieved by using constitutive promoters for transcription factor expression such as the PGK- or EF1 α -promoter. Moreover, it has been demonstrated that significant leaky expression may occur following random genomic integration of the inducible (i) TRE-promoter or by placing the i-TRE in close vicinity to a strong constitutive promoter.

(b) An optimal gene delivery system for forward programming renders the reprogramming factors immune to endogenous silencing mechanisms. Acute viral transduction of hPSCs invariably leads to transgene silencing in a large proportion of transfected cells. This proportion can be reduced by including an antibiotic resistance gene to allow for positive selection of successfully transduced cells. However, the expression levels of these genes required for antibiotic resistance are typically orders of magnitudes smaller than expression levels of reprogramming factors required for the initiation of a successful conversion process. Therefore, in this case, positive selection does not accurately predict successful conversion.

(c) An optimal gene delivery system for forward programming enables very high transgene expression levels to facilitate a successful conversion process (see Fig. 3I-J). Transgene expression levels are a direct function of the strength of the promoter and the effects of silencing/variegation mechanisms, which occur in an integration site-dependent manner.

(d) An optimal gene delivery system for forward programming ensures that all successfully reprogrammed cells are genetically identical and free of genomic alterations that potentially interfere with target cell function.

(e) An optimal gene delivery system for forward programming does not rely on optimization of protocols for the production and titration of lentiviral vectors and the subsequent transduction of hPSCs, which represent a traditionally difficult to transduce cell type.

(f) An optimal gene delivery system for forward programming allows full predictability and reproducibility of the resulting forward programming protocol among different labs and users. Naturally, this is impossible to achieve if the protocol relies on the selection of a clonally expanded line with a randomly integrated transgene. Moreover, it is also difficult to achieve when hPSC-transduction protocols with highly-concentrated lentiviral vectors are required.

Supplemental Movies

Movie S1. Related to Figure 2. Time-lapse of neuron induction

Movie S2. Related to Figure 3. Time-lapse of myocyte induction

Movie S3. Related to Figure 3. Response of induced myocytes to ACh-Receptor stimulation

Supplemental Experimental Procedures

hPSC maintenance culture and germ layer differentiation

Feeder- and serum-free hESC (H9 line; WiCell) and hiPSC (Cheung et al. 2012) culture was performed as previously described (Vallier 2011). Briefly, cells were plated on gelatin/MEF media-coated culture dishes [MEF-media consists of Advanced DMEM/F12 (90%, Gibco), fetal bovine serum (10%, Gibco), L-Glutamine (1mM, Gibco), 2-Mercaptoethanol (0.1mM, Sigma-Aldrich) and Penicillin/Streptomycin (1%, Gibco)], and cultured in chemically defined media [CDM, consisting of IMDM (50%, Gibco), F12 (50%, Gibco), concentrated lipids (100x, Gibco), monothioglycerol (450 μ M, Sigma-Aldrich), insulin (7 μ g/ml, Roche), transferrin (15 μ g/ml, Roche), bovine serum albumin fraction V (5mg/ml, Europa Bioproducts), and Penicillin/Streptomycin (1%)] supplemented with Activin-A (10ng/ml) and FGF2 (12ng/ml; both from Marko Yvonen, Department of Biochemistry, University of Cambridge). Cells were passaged in small clumps using collagenase every 5-6 days.

Differentiation of hPSCs into the germ layers was induced in adherent hESC cultures in accordance to previously published directed differentiation protocols. Briefly, definitive endoderm was derived by culturing hPSCs for 3 days in CDM-PVA (without insulin) supplemented with FGF2 (20ng/ml), Activin-A (100ng/ml), BMP4 (10ng/ml, Marko Hyvonen, Dept. of Biochemistry, University of Cambridge), and LY-294002 (10 μ M, Promega) (Touboul et al. 2010). For derivation of neuroectoderm, hPSCs were cultured for 6 days in CDM-BSA supplemented with SB-431542 (10 μ M, Tocris), LDN-193189 (0.1 μ M, Tocris) and RA (0.1 μ M, Sigma) (Douvaras et al. 2014). Lateral plate mesoderm was obtained by culturing hPSCs for 36h in CDM-PVA supplemented with FGF2 20ng/ml, BMP4 (10ng/ml; R&D), and LY294002 (10 μ M), and for 3.5 subsequent days in CDM-PVA supplemented with FGF2 (20ng/ml) and BMP4 (50ng/ml) (Cheung et al. 2012).

Gene targeting constructs and molecular cloning

We recently described the design and construction of the hROSA26 gRNA/Cas9n expression plasmids and of the hROSA26 targeting vector, and demonstrated that this targeting strategy allows for homogeneous, strong and stable expression of targeted transgenes in hPSCs and their differentiated progenies (Bertero et al. 2016). The pR26_CAG-rtTA targeting vector was constructed by cloning the coding sequence of a third generation rtTA (Zhou et al. 2006) (PCR-amplified from pLVX-Tet3G) into the BamHI/MluI sites of pR26_CAG-EGFP (Bertero et al. 2016) thus replacing the EGFP sequence.

AAVS1 ZFN expression plasmids were a generous gift of Dr. Kosuke Yusa, Wellcome-Trust Sanger Institute (Bertero et al. 2016). The inducible EGFP AAVS1 targeting vector was constructed by Gibson Assembly (New England Biolabs) in which three inserts were ligated into the EcoRI/HindIII sites of the multiple cloning site of the pUC19 vector (Thermo Fisher Scientific): The first insert comprised the upstream AAVS1 homology arm, a splice acceptor, a T2A-site and the puromycin resistance cassette (all these elements were PCR-amplified from pTRE-EGFP; addgene 22074, deposited by Rudolf Jaenisch). The second insert contained the inducible TRE3G promoter (PCR-amplified from pLVX-TRE3G). The third insert comprised the EGFP expression cassette and the AAVS1 downstream homology arm (PCR-amplified from pTRE-EGFP; addgene 22074, deposited by Rudolf Jaenisch). The resulting plasmid was termed pAAV_TRE-EGFP. The pAAV_TRE-NGN2 and pAAV_TRE-MYOD1 targeting vectors were constructed by cloning the NGN2 and MYOD1 coding sequence, respectively (NGN2: PCR-amplified from pLVX-TRE-NGN2 (Ladewig et al. 2012), gift from Oliver Brüstle; MYOD1, OLIG2, SOX10: PCR-amplified from commercially available cDNA plasmids, Open Biosystems) into the SpeI/EcoRI sites of pAAV_TRE-EGFP, thus replacing the EGFP sequence.

Gene targeting

Targeting of the hROSA26 locus (Irion et al. 2007) was performed by nucleofection. Human PSCs were dissociated to single cells with TrypLE Select (Gibco), and 2×10^6 cells were nucleofected (100 μ l reaction volume; total of 12 μ g of DNA, which was equally divided between the two gRNA/Cas9n plasmids and the targeting vector) using the Lonza P3 Primary Cell 4D-Nucleofector X Kit and cycle CA-137 of the Lonza 4D-Nucleofector System. Nucleofected hPSCs were plated onto irradiated multi-drug resistant (DR4) mouse embryonic fibroblasts and cultured in KSR media [consisting of Advanced DMEM/F12 (80%), knock-out serum replacer (20%, Gibco), L-Glutamine (1mM), 2-Mercaptoethanol (0.1mM) and Penicillin/Streptomycin (1%)] supplemented with FGF2 (4ng/ml). Y-27632 (5 μ M, Tocris) was added for 24h before and after nucleofection to promote cell survival. After 3-6 days, neomycin-resistant hPSCs were selected by adding G418 (50 μ g/ml, Sigma-Aldrich) for 7-10 days.

Subsequently, individual clones were picked, expanded in feeder-free conditions and finally analyzed by genotyping.

Targeting of the AAVS1 locus (Hockemeyer et al. 2009) was performed by lipofection. Human PSCs were seeded in feeder-free conditions in 6-well plates, and transfected 48h after passaging. Transfection was performed in Opti-MEM (Gibco) supplemented with Lipofectamine2000 (10 μ l/well, Thermo Fisher Scientific) and a total of 4 μ g of DNA (equally divided between the two AAVS1 ZFN plasmids and the targeting vector) for 24h. After 3-5 days, resistant hPSCs were selected by adding puromycin (1 μ g/ml, Sigma-Aldrich) for 5-8 days. Subsequently, individual clones were picked, expanded and analyzed by genotyping.

Drug-resistant hPSC clones from targeting experiments were screened by genomic PCR to verify site-specific transgene integration, to determine the number of targeted alleles, and to exclude off-target integrations. PCRs were performed with LongAmp Taq DNA Polymerase (New England Biolabs). The primer combinations used for the various targeting vectors are reported in supplemental experimental procedures. The results of all targeting experiments are summarized in Supplemental Table 1. Karyotype analysis was performed by standard G banding techniques (Medical Genetics Service, Cambridge University Hospitals). To prepare the targeted human PSCs for chromosome analysis, cells were incubated in fresh culture media supplemented with Y-27632 (5 μ M, Tocris) and KaryoMAX Colcemid (100ng/ml, Gibco) for 4h at +37°C. Subsequently, cells were harvested as single cells, washed, and pelleted. Nuclei swelling and spreading of the chromosomes was achieved by treatment with hypotonic 0.055 M KCl-solution for 5 minutes. Finally, cells were fixed and preserved in methanol and glacial acetic acid (ratio 3:1).

Induction of neurons

Pluripotent NGN2 OPTi-OX cells were dissociated into single cells with TrypLE and plated onto Matrigel (35 μ g/cm², Scientific Laboratory Supplies) coated dishes at a density of 75.000 cells per well of a 12-well plate. Forward programming was initiated 24 hours after the split. The induction was performed in DMEM/F12 (Gibco) supplemented with Glutamax (100x, Gibco), Non-Essential Amino Acids (100x, Gibco), 2-Mercaptoethanol (50 μ M), Penicillin/Streptomycin (1%), and dox (1 μ g/ml). After 2 days of induction, the medium was switched to Neurobasal-medium supplemented with Glutamax (100x), B27 (50x, Gibco), BDNF (10 ng/ml, Peprotech), NT3 (10 ng/ml, R&D Systems), Penicillin/Streptomycin (1%), and dox (1 μ g/ml). These culture conditions were based on previously described chemically-defined neuronal basal culture media (Zhang et al. 2013), and used for all experiments presented. Cells were cultured for 7-14 days before analysis.

Induction of skeletal myocytes

Pluripotent OPTi-MYOD1 cells were dissociated into single cells with TrypLE and plated onto gelatine/MEF-medium coated dishes at a density of 100.000 cells per well of a 12-well plate. Forward programming was initiated 24 hours after the split. Unless stated otherwise, the induction was performed in DMEM (Sigma-Aldrich) supplemented with L-Glutamine (2mM), 2-Mercaptoethanol (50 μ M), Penicillin/Streptomycin (1%), insulin (7 μ g/ml), all-trans retinoic acid (1 μ M, Sigma-Aldrich), and doxycycline (1 μ g/ml). After 5 days of induction, the medium was supplemented with CHIR99021 (3 μ M, Tocris) and heat-inactivated horse serum (2%, Gibco) to enhance maturation of the induced myocytes as previously described (Abujarour et al. 2014). Unless stated otherwise, these culture conditions were used in all experiments described in this paper. Additional reagents were tested during protocol optimization (see Fig. S2): DMEM/F12 (Gibco), IMDM (Gibco), DMEM (Sigma), α -MEM (Sigma), BMP4 (10ng/ml, Marko Hyvonen, Dept. of Biochemistry, University of Cambridge), cAMP (1 μ M, Sigma), Forskolin (20ng/ μ l, Tocris), IWR-1 (1 μ M, Tocris), LY-294002 (10 μ M), Purmophamine (1 μ M, Tocris), PD-0325901 (1 μ M, Tocris), LDN-193189 (0.1 μ M, Tocris), SB-431542 (10 μ M, Tocris), 9-cis RA (1 μ M, Sigma) TTNPB (1 μ M, Tocris), BMS753 (1 μ M, Tocris), CD2314 (1 μ M, Tocris), BMS961 (1 μ M, Tocris).

Induction of oligodendrocytes

Pluripotent OLIG2-2A-SOX10 OPTi-OX hPSCs were grown in colonies on gelatine/MEF coated culture dishes. Before the start of induction, they were treated with SB and LDN overnight. The following day induction was initiated in CDM supplemented with dox (1 μ g/ml) and RA (0.1 μ M). One day after induction, cells were split in CDM supplemented with RA (0.1 μ M), PM (1 μ M), and Y-27632 (5 μ M), PDGFaa (20ng/ml, Peprotech), FGF2 (5ng/ml) onto PDL/laminin coated culture dishes (100.000 cells per well of a 12 well-plate). The following day cells were switched to oligodendrocyte

media consisting of DMEM/F12, supplemented with Glutamax (100x), Non-Essential Aminoacids (100x), 2-Mercaptoethanol (1000x), Penicillin-Streptomycin (100x), N2 Supplement (100x), B27 Supplement (50x), Insulin 7 μ g/ml (Marko Hyvonen), T3 60ng/ml (Sigma), Biotin 100ng/ml (Sigma), and db-cAMP 1 μ M (Sigma). Oligodendrocyte medium was supplemented with dox (1 μ g/ml), PDGF α (20 ng/ml), FGF2 (5 ng/ml), RA (0.1 μ M) and PM (1 μ M). Seven days post induction RA and PM was withdrawn. To keep induced cells in a proliferative state, cells were passaged every 4 days (75,000 cells per well of a 24-well plate) in the continued presence of the mitogens PDGF α and FGF2. For differentiation of proliferative oligodendrocyte precursors, PDGF α and FGF2 were withdrawn. Human recombinant NT3 (5ng/ μ l, R&D Systems) was added to enhance cell survival.

Quantitative real-time PCR (qPCR)

RNA was extracted using the GenElute Mammalian Total RNA Miniprep Kit and the On-Column DNase I Digestion Set (Sigma-Aldrich). cDNA synthesis was performed with the Maxima First Strand cDNA Synthesis Kit (Thermo Fisher Scientific). Applied Biosystems SYBR Green PCR Master Mix was used for qPCR. Samples were run on the Applied Biosystems 7500 fast PCR machine. All samples were analyzed in technical duplicates and normalized to the house-keeping gene Porphobilinogen Deaminase 1 (*PBGD*). Results were analyzed with the $\Delta\Delta$ Ct method. See supplemental experimental procedures for a full list of primer sequences.

Flow cytometry

For analysis of EGFP expression cells were harvested with TrypLE Select (Gibco) for 5-10 minutes at 37°C to obtain a single cell suspension. Following a wash with PBS, cells were resuspended in ice-cold PBS supplemented with DAPI (10 μ g/ml), and incubated for 5 minutes on ice. Cells were analyzed using a Cyan ADP flow-cytometer to determine the levels of EGFP expression of viable cells (DAPI negative). EGFP levels in non-induced (not dox-treated) iEGFP cells were indistinguishable from wild-type cells and served as negative control. FITC (EGFP) acquisition settings were set to enable plotting of the highest levels of EGFP expression. Thus, the negative control (wild-type and/or uninduced iEGFP cells) is in some instances located directly adjacent to the left y-axis. For staining and analysis of myosin heavy chain expression, cells were harvested with TrypLE Select (as for EGFP expression analysis), washed once with PBS, and fixed and permeabilized with Cytotfix/Cytoperm solution (BD Biosciences). Subsequently, cells were washed and blocked in Perm/Wash buffer (BD Biosciences) supplemented with 3% bovine serum albumin (BSA) at +4°C overnight. Staining with a PE-conjugated anti-MYH antibody (supplemental experimental procedures) was carried out in Perm/Wash buffer for 1h at +4°C in the dark. After three washes with Perm/Wash buffer cells were analyzed with a Cyan ADP flow-cytometer to determine the levels of MHC expression. Induced myocytes stained with an IgG2b isotype-control antibody served as negative control for gating purposes. Stained non-induced iMYOD1 OPTi-OX hPSCs served as experimental negative control. Data analysis was performed with FlowJo (v10) and Graphpad Prism (v6).

Western blot

Whole-cell protein was extracted with CellLytic M (Sigma-Aldrich) supplemented with complete Protease Inhibitor (Roche), and subsequently quantified by using Protein Quantification Kit-Rapid (Sigma-Aldrich). Protein electrophoresis was performed with NuPAGE LDS Sample Buffer and 4-12% NuPAGE Bis-Tris Precast Gels (Invitrogen). Following protein transfer on PVDF, membranes were blocked with PBS supplemented with 0.05% Tween-20 (PBST) 4% milk for 1h at room temperature, and incubated with primary antibodies overnight in PBST 4% milk. Membranes were washed with PBST, incubated with HRP-conjugated secondary antibodies (Sigma-Aldrich) in PBST 4% milk, incubated with Pierce ECL2 Western Blotting Substrate (Thermo Fisher Scientific), and exposed to X-Ray Super RX Films (Fujifilm).

Immunocytochemistry

Cells were fixed in 4% paraformaldehyde (diluted in PBS) for 20 minutes at room temperature and subsequently washed three times with PBS. The cells were then blocked with 10% donkey serum (Sigma-Aldrich) and permeabilized with 0.3% Triton X-100 (diluted in PBS) for 20 minutes at room temperature. Subsequently, cells were incubated with appropriately diluted primary antibodies (supplemental experimental procedures) in 2% donkey serum and 0.1% Triton X-100 (diluted in PBS) at 4°C overnight. Triton-X was omitted throughout all steps when staining the surface antigen PDGFRA, A2B5, and O4. After three washes with PBS, the cells were incubated for 1 hour at room temperature with corresponding donkey fluorophore-conjugated secondary antibodies (Alexa Fluor 488, 555, 568, and/or 647) in PBS supplemented with 1% donkey serum. Nuclei were visualized with

4',6-diamidino-2-phenylindole (DAPI, Thermo Fisher Scientific). EGFP expression and immunostainings were imaged using a Zeiss LSM 700 confocal microscope (Leica). The percentage of β III-tubulin positive cells was calculated by determining β III-tubulin expression in at least 50 randomly selected DAPI-positive cells in 3 visual fields of 3 biological replicates using an inverted Olympus IX71 fluorescence microscope.

Statistical analysis

Statistical analysis was performed with GraphPad Prism (v6). The number of replicates, the statistical test used, and the test results are described in the figure legends. Unless stated otherwise data is presented as mean \pm SEM.

List of primers for genotyping PCR

Locus	PCR type	Primer binding site	Primer sequence
hROSA26	Locus PCR	Genome (5')	GAGAAGAGGCTGTGCTTCGG
		Genome (3')	ACAGTACAAGCCAGTAATGGAG
	5'-INT PCR	Genome (5')	GAGAAGAGGCTGTGCTTCGG
		Splice Acceptor	AAGACCGCGAAGAGTTTGTCC
	3'-INT PCR	rtTA	GAAACTCGCTCAAAAGCTGGG
		Genome (3')	ACAGTACAAGCCAGTAATGGAG
	3'-BB PCR	rtTA	GAAACTCGCTCAAAAGCTGGG
		Vector Backbone (3')	TGACCATGATTACGCCAAGC
AAVS1	Locus PCR	Genome (5')	CTGTTTCCCCTTCCCAGGCAGGTCC
		Genome (3')	TGCAGGGGAACGGGGCTCAGTCTGA
	5'-INT PCR	Genome (5')	CTGTTTCCCCTTCCCAGGCAGGTCC
		Puromycin	TCGTGCGGGTGGCGAGGCGCACCG
	3'-INT PCR	Transgene	transgene specific sequence
		Genome (3')	TGCAGGGGAACGGGGCTCAGTCTGA
	3'-BB PCR	Transgene	transgene specific sequence
		Vector Backbone (3')	ATGCTTCCGGCTCGTATGTT

List of primers for quantitative PCR

Gene	Orientation	Primer sequence
<i>CNP</i>	Fw	TCCTCATCATGAACAGAGGCTT
	Rev	AAACTGCAGCTCAGGCTTGT
<i>CSPG4</i> (<i>NG2</i>)	Fw	GTCGAGGACACCTCCGTTT
	Rev	GTGGTCAGCAGAGAGGACAC
<i>DES</i>	Fw	CCAACAAGAACAACGACGCC
	Rev	ATCAGGGAATCGTTAGTGCCC
<i>DMD</i>	Fw	TGGTGGGAAGAAGTAGAGGACT
	Rev	TGCTGCTTCCAAACTTAGA
EGFP	Fw	CCCGACAACCACTACCTGAG
	Rev	GTCCATGCCGAGAGTGATCC
<i>FOXP1</i>	Fw	TGCCAAGTTTACGACGGGA
	Rev	GGGTTGGAAGAAGACCCCTG
<i>GRIA4</i>	Fw	GGCCAGGGAATTGACATGGA
	Rev	AACCAACCTTTCTAGGTCCTGTG
<i>HMBS</i> (<i>PBGD</i>)	Fw	ATTACCCCGGAGACTGAAC
	Rev	GGCTGTTGCTTGACTTCTC
<i>MAG</i>	Fw	CAGAAGACGTCCCAACTCA
	Rev	CCTCGGGAGGCTGAAATCATAA
<i>MAP2</i>	Fw	AGACTGCAGCTCTGCCTTAG

	Rev	AGGCTGTAAGTAAATCTTCCTCC
<i>MBP</i>	Fw	TGGTGATGGAGATGTCAAGCAGGT
	Rev	GCTGTGGTTTGGAAACGAGGTTGT
<i>MOG</i>	Fw	AGAGATAGAGAATCTCCACCGGA
	Rev	TGATCAAGGCAACCAAGGGTC
<i>MYH1</i>	Fw	CACACTAGTTTCACAGCTCTCG
	Rev	CAGGGCACTCTTGGCCTTTA
<i>MYH2</i>	Fw	GGAAGCTCTGGTGTCTCAGTT
	Rev	CAGGGCGTTCTTGGCTTTTAT
<i>MYH3</i>	Fw	GCTGCATACCCAGAACACCA
	Rev	CCCTGCTGGCATCTTCTACC
<i>MYH4</i>	Fw	TCGCATTTGTCAGCCAAGGG
	Rev	TGAAACCCAGGATGTCCACAG
<i>MYH7</i>	Fw	GAGACTGTCTGGGCTTGT
	Rev	GCCCTTCTCAATAGGCGCATC
<i>MYH8</i>	Fw	TGAAGCAGATAGCAGCGCGA
	Rev	CGTACGAAGTGAGGGTGTGT
<i>MYOD1</i> (endo)	Fw	GCCGCTTTCCTTAACCACAA
	Rev	CTGAATGCCCACTGTC
<i>MYOD1</i>	Fw	CGACGGCATGATGGACTACA
	Rev	TAGTAGGCGCCTTCGTAGCA
<i>NANOG</i>	Fw	AGCAGATGCAAGAACTCTCCAA
	Rev	TGAGGCCTTCTGCGTCACAC
<i>NEUROG2</i> (<i>NGN2</i>)	Fw	TGTTTCGTCAAATCCGAGACCT
	Rev	CGATCCGAGCAGCACTAACA
<i>NKX2.2</i>	Fw	GCTTCCTGCGTCCATTTCCG
	Rev	GAAAGAACTGGGGATGGGGAG
<i>OLIG1</i>	Fw	TGTCGCAGAGAGTTTTCGCT
	Rev	ATGCAAGGCGGTTGGTTTTTC
<i>OLIG2</i>	Fw	ATCGCATCCAGATTTTCGG
	Rev	CCCCAGGGGAAGATAGTCGT
<i>PAX6</i>	Fw	CGAGATTTCAAGAGCCCCATA
	Rev	AAGACACCACCGAGCTGATT
<i>PDGFRA</i>	Fw	AGGGATAGCTTCTGAGCCA
	Rev	AGCTCCGTGTGCTTTCATCA
<i>PLP</i>	Fw	AACAGCTGAGTTCCAAATGACC
	Rev	ACGGCAAAGTTGTAAGTGGC
<i>POU3F2</i> (<i>BRN2</i>)	Fw	ACCCGCTTATCGAAGGCAA
	Rev	CCTCCATAACCTCCCCAGA
<i>POU5F1</i> (<i>OCT4</i>)	Fw	GTGGAGGAAGCTGACAACAA
	Rev	ATTCTCCAGGTTGCCTCTCA
<i>RYR1</i>	Fw	CAATCGCCAGAACGGAGAGA
	Rev	GTCGTGTTCCCTGTCTGTGT
<i>SLC17A6</i> (<i>VGLUT2</i>)	Fw	GTAGACTGGCAACCACCTCC
	Rev	CCATTCCAAAGCTTCCGTAGAC
<i>SOX10</i>	Fw	ACACCTTGGGACACGGTTTT
	Rev	GTCCAACGCCACCTCC
<i>SYP</i>	Fw	ACCTCGGGACTCAACACCTCGG
	Rev	GAACCACAGGTTGCCGACCCAG
<i>SYN1</i>	Fw	CCCTGGGTGTTGCCAGAT
	Rev	ACCACGGGTACGTTGTA
<i>TUBB3</i>	Fw	CAACCAGATCGGGGCCAAGTT
	Rev	CCGAGTCGCCACGTAGTT

List of antibodies

Antigen	Species	Isotype	Clonality	Company	Cat. No.	Dilution
A2B5	mouse	IgM	monoclonal	Millipore	MAB312	1:300
ACTN2 (α -actinin)	mouse	IgG1	monoclonal	Sigma	A7811	1:200
BrdU	mouse	IgG1	monoclonal	BD Bio	347580	1:100
CNP	mouse	IgG1	monoclonal	Abcam	ab6319	1:500
DES (desmin)	rabbit	IgG	monoclonal	Abcam	ab32362	1:500
EOMES	rabbit	IgG	polyclonal	Abcam	ab23345	1:200
MAG	mouse	IgG1	monoclonal	Abcam	ab89780	1:400
MAP2	mouse	IgG1	monoclonal	Sigma	M4403	1:200
MBP	rat	IgG2a	monoclonal	Millipore	MAB386	1:200
MYOD1	rabbit	IgG	monoclonal	Abcam	ab133627	1:250
MYOG (myogenin)	mouse	IgG1	monoclonal	DSHB	F5D	1:100
MYOG (myogenin)	rabbit	IgG	monoclonal	Abcam	ab124800	1:500
MYH (myosin heavy chains)	mouse	IgG2b	monoclonal	DSHB	MF20	1:100
MYH-PE	mouse	IgG2b	monoclonal	BD Biosc.	564408	1:20 (Flow)
NANOG	goat	IgG	polyclonal	R&D	AF1997	1:200
NCAM	mouse	IgG1	monoclonal	DSHB	5.1H11	1:100
NEFH (neurofilament)	rabbit	IgG	polyclonal	Abcam	ab8135	1:1000
NEUROG2 (NGN2)	rabbit	IgG	Polyclonal	Santa Cruz	sc-50402	1:100
NKX2.5	rabbit	IgG	polyclonal	Santa Cruz	sc14033	1:200
O4	mouse	IgM	monoclonal	R&D	MAB1326	1:1000
OCT4	mouse	IgG2b	monoclonal	Santa Cruz	sc5279	1:200
PAX3	mouse	IgG2a	monoclonal	DSHB	Pax3	1:100
PAX6	mouse	IgG1	monoclonal	DSHB	PAX6	1:100
PAX7	mouse	IgG1	monoclonal	DSHB	PAX7	1:100
PLP	rabbit	IgG	monoclonal	Abcam	Ab183493	1:2000
SLC17A7 (VGLUT1)	goat	IgG	polyclonal	Abcam	ab104899	1:500
TNNT2 (troponin T)	mouse	IgG2a	monoclonal	DSHB	CT3	1:100
TTN (titin)	mouse	IgM	monoclonal	DSHB	9D10	1:100

TetR (tet repressor)	mouse	IgG1	monoclonal	Clontech	631131	1:1000 (WB)
TUBA4A (α 4-tubulin)	mouse	IgG1	monoclonal	Sigma	T6199	1:10000 (WB)
TUBB3 (β III-tubulin)	mouse	IgG1	monoclonal	Millipore	MAB1637	1:1000

Supplemental References

- Cheung, C. et al., 2012. Generation of human vascular smooth muscle subtypes provides insight into embryological origin-dependent disease susceptibility. *Nature Biotechnology*, 30(2), pp.165–173.
- Irion, S. et al., 2007. Identification and targeting of the ROSA26 locus in human embryonic stem cells. *Nature biotechnology*, 25(12), pp.1477–82.
- Ladewig, J. et al., 2012. Small molecules enable highly efficient neuronal conversion of human fibroblasts. *Nature methods*, 9(6), pp.575–8.
- Pang, Z.P. et al., 2011. Induction of human neuronal cells by defined transcription factors. *Nature*, 476(7359), pp.220–3.
- Touboul, T. et al., 2010. Generation of functional hepatocytes from human embryonic stem cells under chemically defined conditions that recapitulate liver development. *Hepatology*, 51(5), pp.1754–65.
- Vallier, L., 2011. Serum-free and feeder-free culture conditions for human embryonic stem cells. *Methods in molecular biology*, 690, pp.57–66.
- Zhou, X. et al., 2006. Optimization of the Tet-On system for regulated gene expression through viral evolution. *Gene therapy*, 13(19), pp.1382–1390.